COMMUNICATION

ChemComm
www.rsc.org/chemcomm

Microemulsion-based synthesis of stacked calcium carbonate (calcite) superstructures†

Chulanapa Viravaidya, Mei Li and Stephen Mann*
School of Chemistry, University of Bristol, Bristol, UK BS8 1TS. E-mail: s.mann@bristol.ac.uk; Fax: +44 (0)117 925 1295; Tel: +44 (0)117 331 6797

Received (in Cambridge, UK) 28th May 2004, Accepted 15th July 2004
First published as an Advance Article on the web 16th August 2004

Synthesis of calcium carbonate in water-in-oil microemulsions results in the spontaneous formation of stacked superstructures of 20 nm-thick pseudo-hexagonal calcite plates in crystallographic register.

The synthesis of organized extended structures based on the assembly of nanostructured building blocks is currently recognised as an important theme at the nano–micro interface. A number of strategies have been developed to spatially pattern and control higher-order organization, including chemical and microfabrication methods,[1] and controlled deposition of nanoparticle-based superlattices using solvent evaporation,[2] molecular cross-linking[3] or programmed recognition.[4] Alternatively, recent studies have demonstrated that complex macroscopic structures consisting of self-organized surfactant–inorganic nanofilaments of $BaSO_4$,[5] $BaCrO_4$,[6] $BaCO_3$,[7] $CaSO_4$,[8] or $CaCO_3$[9,10] can be synthesized in water-in-oil microemulsions by emergent processes involving nucleation and growth within aggregates of surfactant-coated amorphous inorganic nanoparticles. The amorphous nanoparticles slowly crystallise within the colloidal aggregates, and because this process is strongly coupled with rearrangement of the surface-adsorbed organic molecules, the resulting nanocrystals exhibit time- and scale-dependent structures and morphologies.[11]

In this communication we report the spontaneous formation of novel complex architectures of the thermodynamically stable calcium carbonate polymorph, calcite, by addition of sodium carbonate-containing NaAOT microemulsions (w = [H_2O]/[surfactant] = 40) to reverse micelles of calcium dodecylbenzenesulfonate under conditions of high alkalinity (pH = 11) and a [Ca^{2+}] : [CO_3^{2-}] molar ratio of 1.4 : 1.† Mixing the microemulsions and reverse micelles gave a clear transparent solution, which slowly turned opaque after 3 h and produced a white macroscopic preciptiate within 24 h. XRD results on the washed precipitate gave distinct sharp reflections with d-spacings of 3.03, 2.49, 2.28, 2.09, 1.91 and 1.60 Å corresponding to the {10.4}, {11.0}, {11.3}, {20.2}, {01.8} and {12.2} Miller indices of well-ordered calcite, respectively. The presence of a broad peak centred at 2θ = 15° corresponding to amorphous calcium carbonate was also detected.[12] FT-IR spectra also confirmed the formation of calcite with characteristic absorption bands observed at 713, 881 and 1413 cm^{-1}, corresponding to the ν_4, ν_2, and ν_3 CO_3^{2-} absorption bands of calcite.[13] Significantly, weak bands were also observed at 2955, 2872, 2926 and 2853 cm^{-1} that were associated with asymmetric and symmetric methyl and methylene C–H stretches, respectively, suggesting that surfactant molecules remained strongly associated with the calcite crystals even after extensive washing. This was consistent with EDX analysis of the superstructures, which showed low intensity peaks at 2.3 keV corresponding to the presence of S.

SEM studies revealed that the precipitated material consisted of stacked arrays of *ca.* 20 nm-thick plate-like calcite crystals with pseudo-hexagonal morphology (Fig. 1). The plates varied in width from around 150 nm at each end of the stack to 1 μm in the central region, to produce a stacked arrangement with bilateral symmetry, suggesting that the superstructures developed within the microemulsion liquid phase and not by uni-directional outgrowth from the walls of the reaction vessel. Moreover, the progressive change in the size of the plates within individual stacks indicated that the plates continued to grow principally in width rather than thickness when interlinked. Although the individual stacks were often disordered and showed extensive curling of the calcite plates possibly due to drying in the SEM, they were structurally intact, suggesting the presence of strong interparticle contacts between adjacent lamellae. Significantly, high magnification SEM images showed close morphological alignment of the pseudo-hexagonal plates (Fig. 2a), as well as a helical pattern of growth steps on the end faces (Fig 2b).

TEM studies showed stacked superstructures viewed predominantly side-on that consisted of disorganized plates, which appeared to be structurally connected by localised interlamellar bridges to produce a spiral assembly of separated calcite nanosheets (Fig. 3a). Corresponding electron diffraction patterns showed rings with superimposed arced reflections (Fig. 3b), consistent with morphological disorder but suggesting some degree of crystallographic coherence between the adjacent lamellae. Electron diffraction patterns recorded from isolated individual plates aligned with their large faces parallel to the substrate surface were indexed as single crystals of calcite viewed along the [001] zone (Fig 3c and d), indicating that the stack direction was parallel to the crystallographic c axis. Significantly, electron diffraction patterns recorded from stacks that consisted of less than four well-defined plate-like lamellae and viewed end-on showed either a single [001] zone pattern or a superimposition of [001] zone patterns that were very closely aligned with an angular deviation of less than 10° †. The data were therefore consistent with a structural model for the stacked arrays in which the calcite plates were aligned along a common crystallographic c axis and co-aligned azimuthally along their a and b axes. TEM investigations on the early stages of development of the stacked superstructures confirmed that the

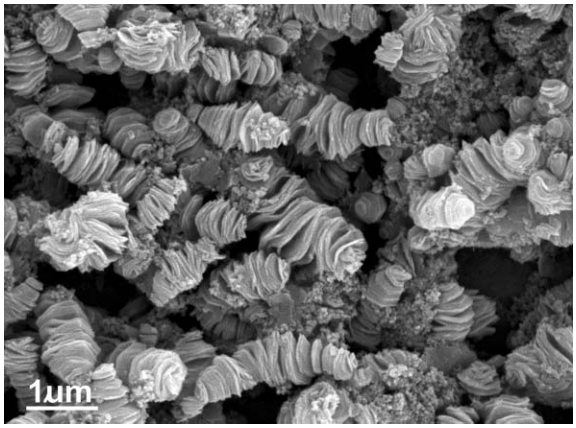

Fig. 1 SEM image showing stacked lamellar calcite superstructures, scale bar = 1 μm.

† Electronic supplementary information (ESI) available: experimental methods, TEM images and corresponding electron diffraction patterns, and SEM image of a stacked lamellar structure formed at w = 20. See http://www.rsc.org/suppdata/cc/b4/b408041f/

DOI: 10.1039/b408041f

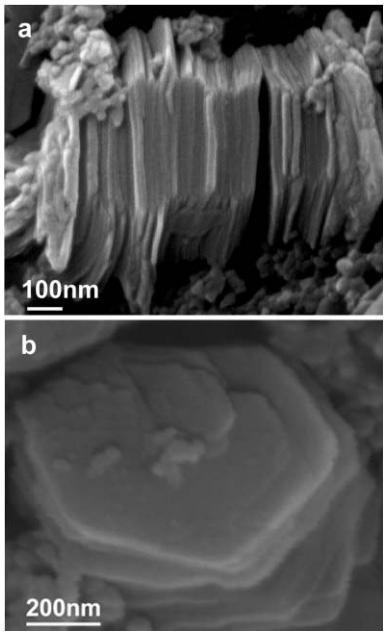

Fig. 2 SEM images of (a) side-view of individual stack showing morphological co-alignment of 20 nm-thick pseudo-hexagonal calcite plates; scale bar = 100 nm; (b) end-view of stack showing spiral growth pattern of surface steps, scale bar = 200 nm.

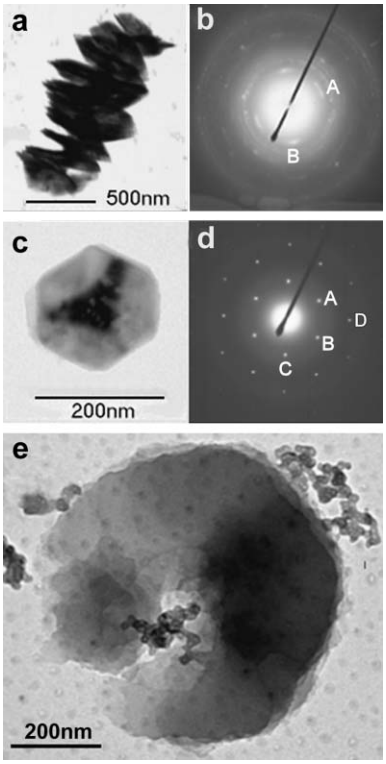

Fig. 3 (a) TEM image of disordered but helically interconnected stack of calcite plates viewed side-on and (b) corresponding electron diffraction data showing ring pattern with superimposed single-crystal reflections such as highlighted by A and B. (c) Top view of an individual calcite plate and (d) the associated [001] zone electron pattern. Reflections A, B, C and D correspond to Miller indices and measured *d* spacings of $(2\bar{1}.0)$ (2.47 Å), (11.0) (2.51 Å), $(\bar{1}2.0)$ (2.51 Å), (30.0) (1.42 Å), respectively; measured interplanar angles: A^C = 60°, A^B = 62°, B^C = 58°. (e) TEM image of a primary plate-like crystal showing spiral outgrowth from {001} faces. Scale bar = 200 nm.

nascent crystals were in the form of discrete calcite plates, which developed by spiral outgrowth from the {001} top and bottom faces (Fig. 3e) to produce the next generation of lamellae.

The results indicate that the stacks develop by helical propagation of surface steps from a primary plate-like single crystal, and not for example by oriented aggregation of preformed calcite tablets. The growth model accounts for the high degree of crystallographic and morphological alignment, as well as the structural integrity of individual stacks when subjected to significant levels of physical stress during sample preparation procedures. Moreover, in order to explain how the helical outgrowth of calcite steps on the {001} faces gives rise to discrete 20 nm-thick inorganic lamellae rather than a consolidated single crystal, we propose that these faces are not only preferentially stabilised by surfactant adsorption but that segmentation occurs during outgrowth from the primary plate due to occlusion of the strongly bound AOT and dodecylbenzenesulfonate molecules to produce a spirally connected lamellar nanocomposite of co-aligned calcite plates interspaced with ultrathin organic sheets, possibly only a single surfactant bilayer in thickness. In support of this model, we note that calcium carbonate crystallization under compressed Langmuir monolayers of *n*-eicosyl sulfate results in nucleation and stabilization of the calcite {001} face due to a combination of stereochemical, geometric and electrostatic matching.[14] In addition, unlike previous studies on the microemulsion-based synthesis and assembly of doughnut-shaped mesoporous particles of interlinked aragonite nanofilaments,[10] the primary calcite plates were not intimately associated with colloidal aggregates of surfactant-capped amorphous calcium carbonate (ACC) nanoparticles. This suggests that the calcite crystals are produced by solution-mediated primary nucleation rather than mesoscale transformation within colloidal aggregates of ACC nanoparticles, and that this distinct change in the mechanism accounts for formation of the thermodynamically stable polymorph and the step-mediated growth process. Indeed, other experiments undertaken at an initial *w* value of 20 rather than 40, produced mixtures of stacked calcite plates and doughnut-shaped aragonite particles (data not shown), consistent with the reduced solubility of ACC nanoparticles under these conditions.

Notes and references

1 P. Yang, A. H. Rizvi, B. Messer, B. F. Chmelka, G. M. Whitesides and G. D. Stucky, *Adv. Mater.*, 2001, **13**, 427.
2 Z. L. Wang, *Adv. Mater.*, 1998, **10**, 13.
3 M. Brust, D. Bethell, D. J. Schiffrin and C. J. Kiely, *Adv. Mater.*, 1995, **7**, 795.
4 C. A. Mirkin, R. L. Letsinger, R. C. Mucic and J. J. Storhoff, *Nature*, 1996, **382**, 607.
5 (*a*) J. Hopwood and S. Mann, *Chem. Mater.*, 1997, **9**, 1819; (*b*) M. Li and S. Mann, *Langmuir*, 2000, **16**, 7088.
6 M. Li, H. Schnablegger and S. Mann, *Nature*, 1999, **402**, 393.
7 L. Qi, J. Ma, H. Cheng and Z. Zhao, *J. Phys. Chem. B*, 1997, **101**, 3460.
8 G. D. Rees, R. Evans-Gowing, S. J. Hammond and B. H. Robinson, *Langmuir*, 1999, **15**, 1993.
9 M. Li and S. Mann, *Adv. Funct. Mater.*, 2002, **12**, 773.
10 M. Li, B. Lebeau and S. Mann, *Adv. Mater.*, 2003, **15**, 2032.
11 H. Cölfen and S. Mann, *Angew. Chem., Int. Ed.*, 2003, **42**, 2350.
12 J. Aizenberg, G. Lambert, L. Addadi and S. Weiner, *Adv. Mater.*, 1996, **8**, 222.
13 S. I. Kuriyavar, R. Vetrivel, C. G. Hegde, A. V. Ramaswamy, D. Chakrabarty and S. Mahapatra, *J. Mater. Chem.*, 2000, **10**, 1835.
14 B. R. Heywood and S. Mann, *Chem. Mater.*, 1994, **6**, 311.